# Energy & Environmental Science

Accepted Manuscript

This article can be cited before page numbers have been issued, to do this please use: M. H. Braga, A. Murchison, J. A. Ferreira, P. Singh and J. B. Goodenough, *Energy Environ. Sci.*, 2015, DOI: 10.1039/C5EE02924D.




ROYAL SOCIETY OF CHEMISTRY

www.rsc.org/ees

View Article Online
DOI: 10.1039/C5EE02924D

**Broader Context Box.**

The development of a glass solid electrolyte conducting either lithium or sodium ions at rates comparable to those of an organic-liquid electrolyte at ambient temperatures through which alkali metals can be reversibly plated/stripped offers the possibility of a safe, high energy-density, lower-cost rechargeable battery for powering an electric vehicle; the preparation of a large-area anode is facile. Moreover, the unusually high dielectric constant of the material may prove useful for electrochemical capacitors and other devices.

View Article Online
DOI: 10.1039/C5EE02924D

# Glass-Amorphous Alkali-Ion Solid Electrolytes and Their Performance in Symmetrical Cells

M. Helena Braga[1], Andrew J. Murchison[1,2], Jorge A. Ferreira[3], Preetam Singh[2], and John B. Goodenough[2],

[1]CEMUC, Engineering Physics Department, Engineering Faculty, University of Porto, R. Dr. Roberto Frias s/n, 4200-465 Porto, Portugal

[2]Texas Materials Institute and the Materials Science and Engineering Program, The University of Texas at Austin, Austin, TX 78712, USA

[3]Energy and Geology National Laboratory (LNEG), R. da Amieira, 4466-901 S. Mamede de Infesta, Portugal

Correspondence to: mbraga@fe.up.pt or jgoodenough@mail.utexas.edu





## Abstract

Precursors of the crystalline antiperovskites $A_{3-x}H_xOCl$ (A = Li or Na and $0 < x < 1$) can be rendered glass/amorphous solid $Li^+$ or $Na^+$ electrolytes by the addition of water to its solvation limit with/without the addition of a small amount of an oxide or hydroxide. The solvated water is evaporated as HCl and $2(OH)^- = O^{2-} + H_2O$. The $O^{2-}$ attracts a $Li^+$ or $Na^+$ to form dipoles; the remaining $Li^+$ or $Na^+$ are mobile. The $Li^+$ or $Na^+$ ionic conductivities of the glass/amorphous solids have activation energies $\Delta H_m < 0.1$ eV and a room-temperature conductivity comparable to that of the best organic liquid electrolytes. Measurements of the dielectric loss tangent versus frequency show two overlapping resonances at room temperature with the Ba-doped Li-glass; they are nearly overlapping at temperatures $41°C < T < 141°C$ in the Ba-doped Na-glass. Galvanostatic charging of a symmetric Cu/Na-glass/Cu cell for 1 h showed a remarkable self-charge on switching to open circuit; charging for 15 h followed by discharging at an applied −0.1 mA of the symmetric cell showed, in the discharge mode, a replating of sodium on the anode at a positive cell current of +0.07 mA for over 15 h. A model for these behaviors is proposed. A symmetric Li/Li-glass/Li cell was cycled to demonstrate plating of Li on a current collector from the Li-glass electrolyte.

View Article Online
DOI: 10.1039/C5EE02924D

View Article Online
DOI: 10.1039/C5EE02924D



## Introduction

The anode of a rechargeable cell for a Li-ion or Na-ion battery continues to plague development of a safe, low-cost battery of sufficient energy density to power an all-electric family car or store sufficient electrical energy generated by solar and/or wind energy. The optimum anode would be lithium or sodium, but plating of these metals on an anode current collector that can be wet by the alkali metal still results in dendrite formation if the plating is done via an organic liquid electrolyte. It has been commonly assumed that dendrites would not be a problem if the plating is done through a solid electrolyte, but this assumption needs to be tested. A first step toward a solution of the anode problem is the development of a low-cost, solid $Li^+$ or $Na^+$ electrolyte that can be fabricated easily to cover a large area as a mechanically robust solid; the next step is to show that $Li^+$ or $Na^+$ ions from the electrolyte can be plated, reversibly and rapidly, as a lithium or sodium anode on a current collector over a long cycle life.

Advanced superionic conduction of $Ag^+$ and $Cu^+$ has been demonstrated in solids that have mobility activation energies $\Delta H_m < 0.1$ eV[1]. In this paper we report experiments on the glass/amorphous solids that exhibit advanced superionic conductivity of $Li^+$ and $Na^+$ ions. Although an alkali-ion anode should not contact water, we demonstrate preliminary results on the reversible plating of a sodium and of a lithium anode, illustrating that the electrolytes are dry alkali-ion conductors although formed by solvating water. The conduction bands of the solid electrolytes have energies far enough above the Fermi energies of metallic lithium and sodium to eliminate formation of a solid-electrolyte interphase (SEI) passivation layer. Present-day Li-ion batteries are fabricated in the discharged state to avoid any alkali metal in the anode, but the anode of a high-voltage cell reacts with the organic-liquid electrolyte used and forms an SEI layer. The passivating SEI layer is necessarily permeable to the working ion, $Li^+$ or $Na^+$, and the working ions in an SEI layer that forms on charge, particularly the initial charge, are robbed irreversibly from the cathode. An alkali-metal anode would give the highest energy density for a given cathode, but plating of a solid alkali-metal anode on charge from a liquid electrolyte is not smooth; dendrites form on preferred crystal faces, and on repeated charges, the dendrites can grow across an organic-liquid or polymer electrolyte to short-circuit the cell with incendiary consequences unless the dendrites are blocked. The dendrites pose a safety issue that has led some people to assume that only an all-solid-state battery can be safe. However, a solid electrolyte in contact with an alkali-metal anode blocks dendrite growth and may even prevent

View Article Online
DOI: 10.1039/C5EE02924D



dendrite formation, thus eliminating the safety issue; and if the solid electrolyte is stable on contact with an organic liquid or polymer electrolyte, a safety problem does not arise with the small amount of organic electrolyte needed to enable higher capacities with a wide range of available cathode strategies, including not only insertion hosts but also both redox-molecule flow-through and sulfur cathodes. The critical remaining question is whether alkali-metal anodes can be plated through a solid electrolyte efficiently at high rates over thousands of charge/discharge cycles.

**Formation of Dry Glass/Amorphous Solids by Water Solvation**

The formation of a dry glass/amorphous $Li^+$ or $Na^+$ solid electrolyte by the solvation of water into a crystalline solid containing $Li^+$ or $Na^+$ ions must involve the separation of $H_2O$ into $(OH)^-$ and $H^+$ ions with the subsequent loss of $H^+$ either by capture by an $O^{2-}$ ion to form $(OH)^-$ anions or by combining with a halide ion, preferably $Cl^-$, to escape the solid as gaseous HCl. The $(OH)^-$ may remain in the solid or react with one another, $2(OH)^- = O^{2-} + H_2O$, with the water leaving as gaseous $H_2O$. Any remaining $(OH)^-$ anions may be captured by an electropositive cation forming a hydrated polyanion. Transformation of the crystalline solid into a glass/amorphous solid may be aided by addition of a small amount of an oxide or hydroxide.

We illustrate this concept by the transformation of the antiperovskite $A_3OCl$ (A = Li or Na) precursors into a glass/amorphous $Li^+$ or $Na^+$ advanced superionic conductor by adding water to its solvation limit with the addition of a small amount of $Ba(OH)_2$ or $Ca(OH)_2$ to lower the glass transition temperature $T_g$ to near room temperature (other oxide or hydroxide additives may also be used). Above $T_g$, a $\Delta H_m < 0.1$ eV for the $Li^+$ or $Na^+$ mobility is obtained. Breaking the dry product into small particles in ethanol results in a paste that can be easily doctor-bladed over a large-area current collector; the paste reforms to the glass with essentially no grain boundaries or pores on evaporation of the ethanol above 130 °C. We demonstrate plating of sodium across a solid-solid interface with a copper current collector in a preliminary investigation of reversible alkali-metal plating across a solid electrolyte. We also demonstrated reversible plating of Li from a Li-glass electrolyte over many cycles in a symmetric Li/Li-glass/Li cell.

View Article Online
DOI: 10.1039/C5EE02924D





## Methods

*Synthesis*. Nominal glass/amorphous solid electrolytes $A_{2.99}M_{0.005}OCl_{1-x}(OH)_x$ with A = Li or Na and M = Ba or Ca were processed from the commercial precursors LiCl (>99 %, Merck) or NaCl (99.9 %, Merck), Li(OH) (98.0 %, Alfa Aesar), or Na(OH) (>99 %, Merck), and $Ba(OH)_2 \cdot 8H_2O$ (98.5 %, Merck), or CaOH (≥ 96.0 %, Merck). From the glass products, HCl is evaporated at lower temperatures and the loss of the $(OH)^-$ by the reaction $2(OH)^- = O^{2-} + H_2O$ occurs above 230 °C as can be seen in Figs 1 and 2; the reaction leaves nearly two $Li^+$ per $Li_{3-x}OCl_{1-x}$ free to move and one $Li^+$ attached to the $O^{2-}$ to form an $(OLi)^-$ dipole. No evidence was found from X-ray diffraction (XRD) for the formation of $Li_2O$. Samples reacted above 230 °C showed a $Li^+$ conductivity two orders of magnitude greater than those annealed below 230 °C.

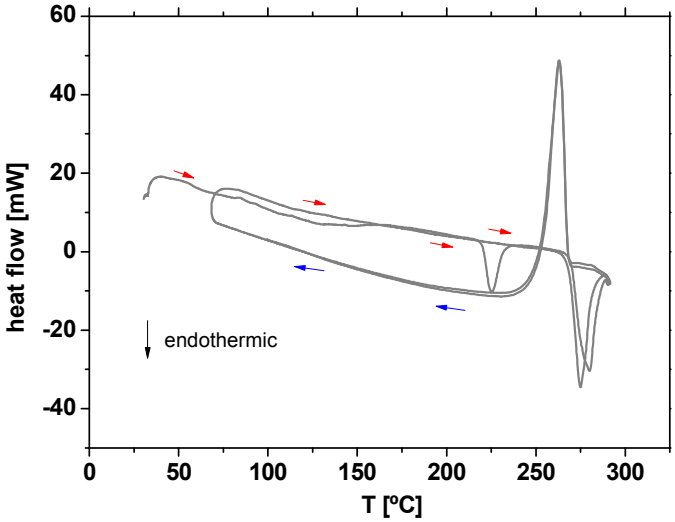


**Fig. 1** Differential Scanning Calorimetry (DSC) of the $Li_3OCl_{1-x}(OH)_x$ at a scanning rate of 5 °C $min^{-1}$ for two heating/cooling cycles. The first cycle while heating shows a glass transition at $T_g$ ≈ 128 °C, the melting point of a hydroxide phase, at 220 °C, and the melting point of the amorphous/glass phase at 269 °C. During cooling the only thermal anomaly observed corresponds to the melting point of the amorphous/glass phase at 269 °C. While heating during the second cycle, only the melting point of the amorphous/glass phase at 269 °C is clearly observed.

The precursors were weighed and mixed in stoichiometric amounts for 25 g batches; 10 to 30 ml of deionized water was added to the powder mixture before the solution was enclosed in a teflon

View Article Online
DOI: 10.1039/C5EE02924D



reactor that was heated to 230 to 250 °C for 2-3 h in a heated sand bath. The hot reactor was then opened to evaporate water and HCl from the glass/amorphous products at the heating temperature. A slurry was prepared by grinding the glass/amorphous product to a powder in liquid ethanol (99.9 %, Merck) to prevent attack of the particle surfaces by humid air. Similar procedures have been described for glass-electrolyte experiments with gold blocking electrodes and alkali-metal electrodes[2]. The XRD data for the glass/amorphous phase has been presented[2]; it shows that nominal crystalline $Li_3OCl$, when mixed with a little $Ba(OH)_2$ and the proper amount of water, transforms to a mostly amorphous product by 180 ºC and a completely amorphous by 230 ºC.

*Cell preparation.* The ethanol slurry was doctor-bladed onto current collectors of copper (Cu) foil. A symmetric cell 1-4 mm thick was made by pressing together the electrolyte faces of two Cu collectors. The cell was then hermetically sealed in a container of Epoxy resin made free of moist air and oxygen; the collector terminals retained an external access. The ethanol evaporated through the Epoxy at 130 to 150 °C leaving a reformed glass/amorphous solid $Li^+$ or $Na^+$ electrolyte free of grain boundaries. The ethanol evaporates through the wet Epoxy layer, which is kept warm by the exothermic reaction of Epoxy formation.

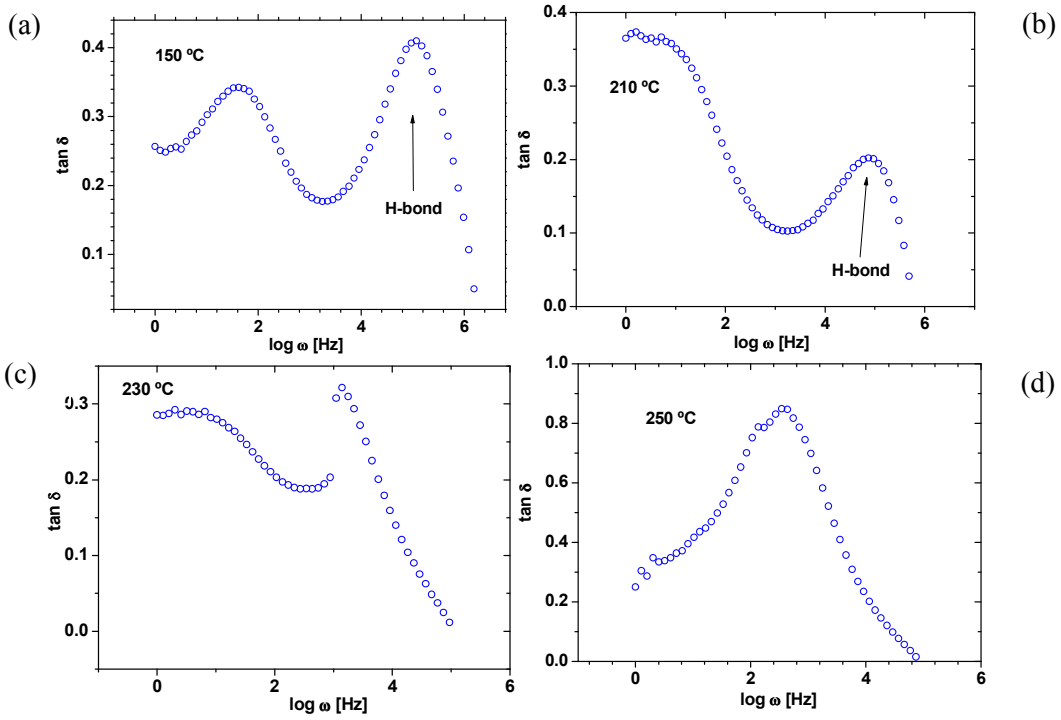

View Article Online
DOI: 10.1039/C5EE02924D



**Fig. 2.** Loss tangent versus frequency of $Li_3OCl_{1-x}(OH)_x$ electrolyte versus temperature for 150 °C ≤ T < 230 °C, (a) - (b), and (c) - (d) at T ≥ 230°C after loss of $(OH)^-$.

*Differential Scanning Colorimetry:* DSC experiments were performed in closed alumina crucibles in an Ar atmosphere flow of 27 mL/min. The synthesized powder was dried before being pressed against the crucible to ensure contact between the product particles. The measuring rate was 5 °C/min, the reference an empty alumina cell, and the instrument was a Setaram Labsys.

*Electrochemical measurements.* Galvanostatic cycling with an SP240 potentiostat (Bio-Logic, France) was performed at 0.2 – 1.8 mA/g from 0 to 10 V versus $Li^+/Li^0$ or $Na^+/Na^0$. Electrochemical impedance spectroscopy was obtained at open-circuit voltage with an AC amplitude of 10 mV over a frequency range from 100 mHz to 5 MHz. Open-circuit voltages after fabrication, charge, and discharge were measured with commercial multimeters.

*Transport characterization.* The ionic conductivities and dielectric loss tangents were obtained with glass-electrolyte plates between blocking gold (Au) electrodes that simulated "ideal" parallel-plate capacitors in which the separation distance *d* between the Au plates of large area A is $d << A$ where Gauss' law applies. With the equivalent circuits described elsewhere[2], the calculated ionic conductivity, $\sigma_i$, obtained from the Nyquist plot is given by

$$R = d/\sigma_i A \quad (1)$$

where R is the measured resistance to the ionic conduction in the glass/amorphous electrolyte.

The relative permittivity measurements may contain responses from interfacial polarization as well as conductivity and electrode polarization; therefore, the electrolyte may give different permittivities as measured on different cells. As a control, we have also calculated the zero-frequency permittivity $\varepsilon_r'$ for a Na-glass electrolyte between two Cu plates; the measured $\varepsilon' = \varepsilon_r'\varepsilon_0$ where $\varepsilon_0$ = 8.54 x $10^{-12}$ $Fm^{-1}$ is the vacuum permittivity. The real and imaginary permittivities $\varepsilon_r'(\omega)$ and $\varepsilon_r''(\omega)$ can then be calculated, respectively, from the measured $\varepsilon_r(\omega) = \varepsilon_r'(\omega) - i\varepsilon_r''(\omega)$ by

$$\varepsilon_r'(\omega) = dZ''/A\varepsilon_0\omega\,(Z'^2 + Z''^2) \quad (2)$$

View Article Online
DOI: 10.1039/C5EE02924D

$$\varepsilon_r''(\omega) = dZ'/A\varepsilon_0\omega\,(Z'^2 + Z''^2) \quad (3)$$

where $\varepsilon_r(\omega) = [\varepsilon_r'^2(\omega) + \varepsilon_r''^2\,(\omega)]^{1/2}$ is the permittivity modulus, ω is the angular frequency, Z′[Ω] and Z″[Ω] are, respectively, the measured real and imaginary impedance. The thickness *d* and area A of a cell were measured after cell assembly.

The dielectric loss tangent (tan δ) was also obtained from

$$\tan\delta = \varepsilon_r''(\omega)/\varepsilon_r'(\omega)$$

to identify resonant frequencies corresponding to different conduction processes.

**Results**

**Fig. 3** Photograph of the glass electrolyte after synthesis

Fig. 3 shows a typical glass/amorphous solid-electrolyte mass after water and gas evaporation in a sand bath. In a humid atmosphere, the mass takes up bound surface water. Therefore, to prepare a slurry, the large mass is first broken into smaller pieces that are placed immediately into ethanol for grinding into small particles within a paste.

View Article Online
DOI: 10.1039/C5EE02924D



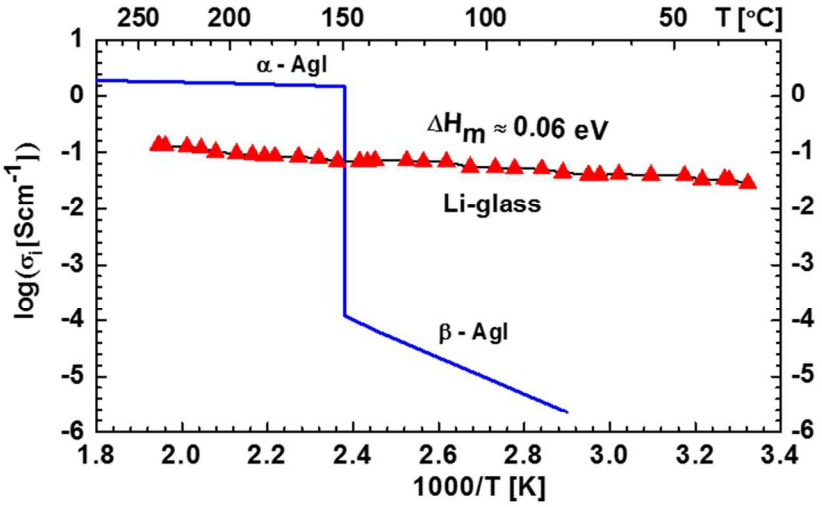


**Fig. 4** Comparison of the Arrhenius plot of the ionic conductivity of the Li-glass with that of AgI.

Fig. 4 compares an Arrhenius plot of the ionic conductivity $\sigma_i$ of AgI (3) with that of a glass pellet of nominal composition $Li_{2.99}Ba_{0.005}OCl_{1-x}(OH)_x$, here after referred to as the Li-glass. From an analysis of the dielectric-loss spectrum, we can conclude it contains no detectable hydrogen bonds. Since there is no evidence of a glass transition temperature above room temperature in Fig. 2, we calculate the activation energy of the ionic mobility from the slope of the Arrhenius plot to be $\Delta H_m \approx 0.06$ eV. The magnitude of $\sigma_i$ at room temperature is seen to be comparable to that of a conventional organic liquid electrolyte.

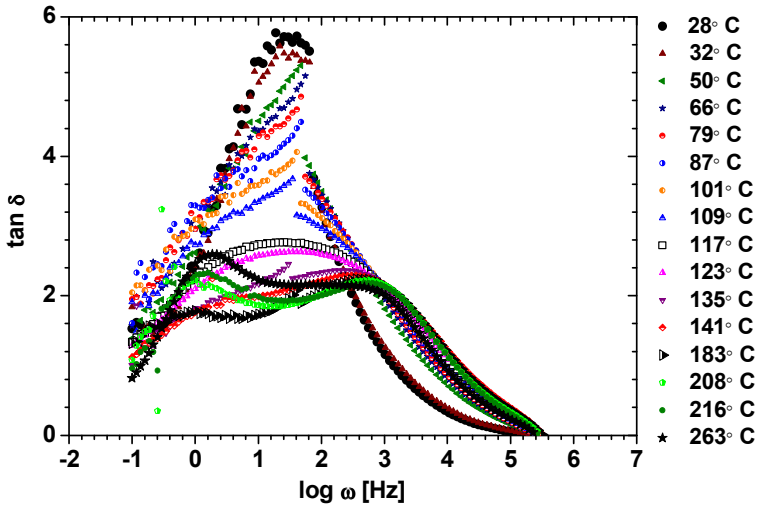


**Fig. 5** Temperature dependence of the Li-glass dielectric-loss tangent versus logarithm of the frequency.

View Article Online
DOI: 10.1039/C5EE02924D



Fig. 5 shows the temperature dependence of the dielectric loss tangent (tan δ) versus the logarithm of the applied frequency, log ω [Hz], of the Li-glass. At 28 °C, the tan δ shows a resonance peak at log ω = 1.4 and a discontinuity at log ω = 1.8 to another resonance at a higher frequency. As the temperature increases, the maximum tan δ occurring at log ω = 1.4 at 28 °C splits into two resonant peaks; two processes having a similar resonance frequency reinforce one another at 28 °C. As the frequency increases, the sharp drop in tan δ at log ω = 1.8 is a decoupling to the high-frequency side of a higher-frequency resonance. As the temperature increases to 123 °C, the two resonances split apart and broaden sufficiently by 117 °C to overlap again; but by 135 °C, they decouple again at log ω ≈ 1.8. By 183 °C, a third resonance is visible at log ω ≈ −0.4; this resonance shifts to higher log ω with increasing temperature to overlap and enhance the lower of the two original resonances at log ω = 0.2 by 263 °C. No resonance corresponding to hydrogen bonds is observed at log ω ≈ 5 to 6.

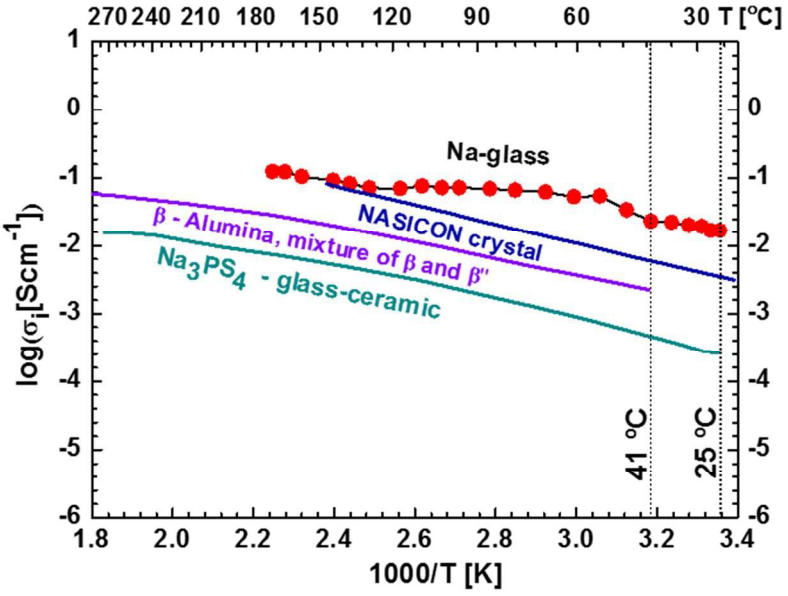


**Fig. 6** Comparisons of the Arrhenius plot of the Na-glass and three other fast $Na^+$-ion electrolytes.

Fig. 6 compares the Arrhenius plot for the nominal composition $Na_{2.99}Ba_{0.005}OCl_{1-x}(OH)_x$, referred to hereinafter as the Na-glass, with those for other Na-ion superionic conductors. In this plot, a glass transition temperature $T_g \approx 41$ °C is manifest with an enhancement $\Delta\sigma_i/(T-T_g)$ of the ionic conductivity in the interval $T_g < T < 140$ °C.

View Article Online
DOI: 10.1039/C5EE02924D



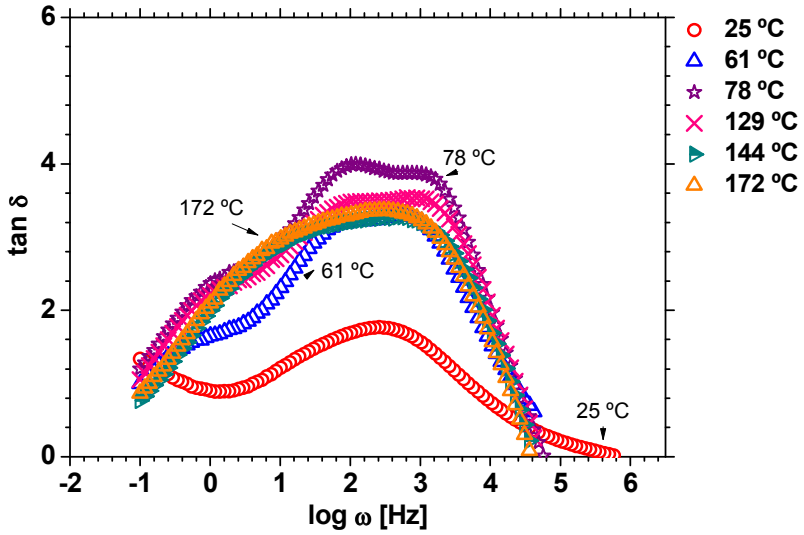


**Fig. 7** Temperature dependence of the Na-glass dielectric-loss tangent versus logarithm of the frequency.

Fig. 7 shows the temperature dependence of the dielectric loss tangent (tan δ) versus log ω. At 25 °C, a broad resonance may be decomposed into two broad resonances with a lower-frequency peak near log ω = 1.4 and the other at a log ω ≈ 2.6. As the temperature increases to T > $T_g$, both resonances increase in amplitude and frequency with a maximum amplitude occurring between 61°C and 129 °C. In the Na-glass, both frequencies have been shifted to higher frequency relative to those found in the Li-glass, and there is no sharp drop in tan δ on going from one resonance to the other. A third resonance of much lower frequency is also present in Fig. 5; its frequency increases with temperature from log ω near −1.0 at 25 °C to > 0.2 at 172 °C. As the low-frequency resonance shifts to higher frequencies with increasing temperatures, it is enhanced by coupling to the mid-frequency resonance.

View Article Online
DOI: 10.1039/C5EE02924D



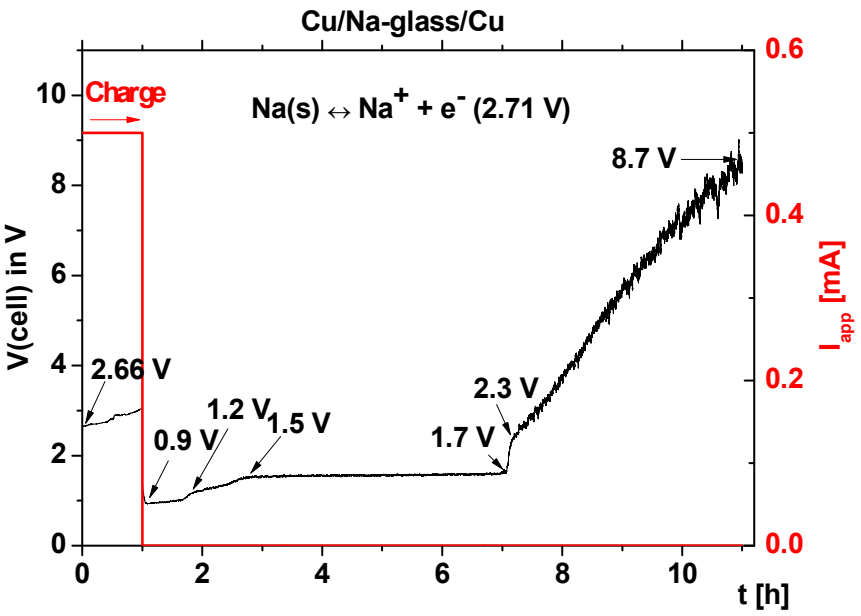


**Fig. 8** Cell charged at a fixed current followed by the open-circuit cell voltage versus time of a symmetric Cu/Na-glass/Cu cell.

Fig. 8 shows the variation over time of the voltage of a symmetric Cu/Na-glass/Cu cell charged with an applied current of 0.5 mA; the measured cell current during charge was 0.65 mA. The cell voltage from 2.66 to 3.0 V during charge indicates plating of Na on the Cu current collector is occurring. After 1 h of charge, the cell was switched to open-circuit and the cell voltage dropped abruptly from 3.0 to 0.9 V. In the open-circuit condition, the cell voltage increased over a period of 2 h from 0.9 to 1.5 V with a small step to 1.2 V after about 1 h; the cell voltage then increased slowly and smoothly to 1.7 V over the next 4 h. Remarkably, 6 h after the circuit was opened, a sharp jump in the self-charge from 1.7 to 2.3 V was followed by a steady increase to 8.7 V over the next 4 h.

View Article Online
DOI: 10.1039/C5EE02924D



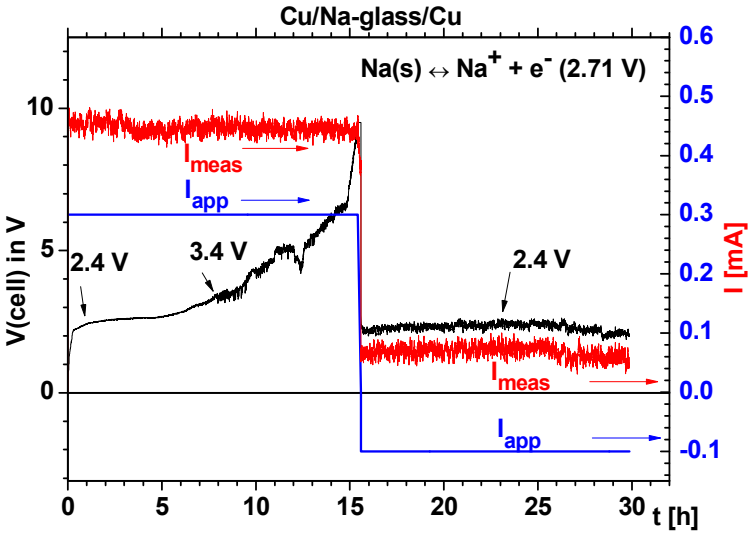


**Fig. 9** Cell voltages and current with an applied charging current of 0.3 mA for 15 h of a symmetric Cu/Na-glass/Cu cell followed by an applied −0.1 mA discharge current and measured cell charging voltage and current for 15 h.

Fig. 9 shows the variation with time of the voltage of another Cu/Na-glass/Cu symmetric cell charged with a fixed applied current of 0.3 mA, but this time for 15 h. In this cell also the measured current during charge was 0.45 mA. During charge, the cell voltage increased from 2.4 to 3.4 V for the first 7 to 8 h, typical of plating of Na on the current collector; but over the next 7 h, the voltage increased more rapidly with time to about 6.5 V before increasing sharply to 9 V after charging for 15 h. The cell was then switched to a cell discharge with a fixed applied current of −0.1 mA, but the measured current remained positive at 0.07 mA with a cell voltage of 2.4 V that also remained relatively stable for the next 15 h with a broad maximum near 10 h.

View Article Online
DOI: 10.1039/C5EE02924D



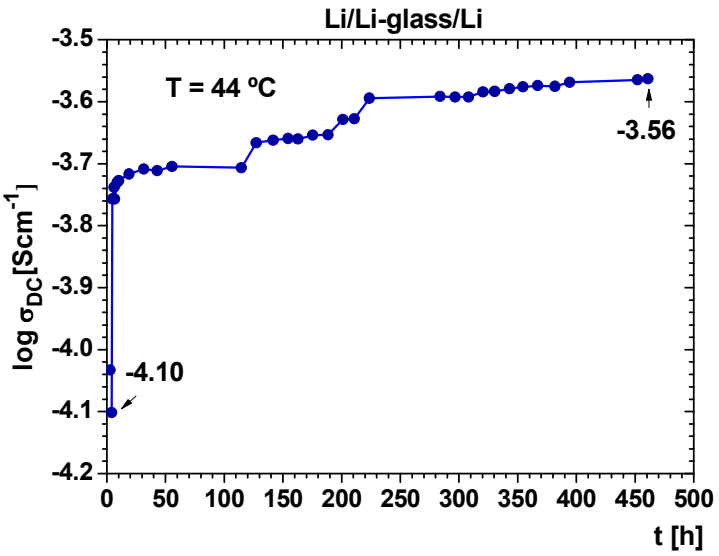


**Fig. 10** Shows the results of chronopotentiometry (a galvanostatic direct current, DC, experiment as described in[2]) on a symmetric Li-metal/Li-glass/Li-metal cell with calcium-doped Li-glass, $Li_{2.99}Ca_{0.005}OCl$. The cell voltage was reversed every 20 min. at a current of 0.10 mA $cm^{-2}$ during 19 days in an argon-filled glove box.

Fig. 10 shows the result of chronopotentiometry (a galvanostatic direct current (DC) experiment described elsewhere[2]) made at 44 °C in an argon-filled glove box on a symmetric Li/Li-glass/Li cell with Ca-doped Li-glass ($Li_{2.99}Ca_{0.005}OCl$).

**Discussion**

The evidence for plating from the Na-glass of metallic sodium onto a Cu current collector in the range 2.4 to 3.4 V during charge of a symmetric Cu/Na-glass/Cu cell, Figs. 8 and 9, indicates that the Na glass is a dry $Na^+$ electrolyte. Similarly, evidence of reversible plating of Li in the symmetric Li/Li-glass/Li cell (Fig. 10) shows the Li-glass is dry. Moreover, Fig. 2 shows the absence of hydrogen bonding above 230 ºC, which indicates $H^+$ ions have been lost has HCl and $(OH)^-$ as water by 230 ºC. With a dry glass, the only mobile species can be $Li^+$ or $Na^+$ and, perhaps, slower moving $(OLi)^-$ and $(ONa)^-$ dipoles.

Both the Li-glass and the Na-glass show two resonances of comparable frequency in their tan δ spectra after the loss of $(OH)^-$, Figs. 2(d), 5, and 7, that reinforce each other where the maximum resonance frequencies overlap. In the Li-glass, the two resonant frequencies overlap at room temperature, and little change in the temperature dependence of the low activation energy of the $Li^+$ mobility is observed in Fig. 4. One of the two resonances must correspond to the energy ħω for a cation hop to a neighboring empty site. Since the other resonance has a similar

View Article Online
DOI: 10.1039/C5EE02924D



frequency and enhances the hopping resonance, it appears to be associated with the hopping process. On raising the temperature, both resonances broaden as the higher-frequency resonance moves to larger log ω; but by 183 °C, a third resonance is visible that also shifts to higher log ω as the temperature increases. At temperatures where the third resonance overlaps the lower of the two original resonances, the overlapping resonances enhance one another. Therefore, we believe the middle of the three resonant frequencies represents the Li hopping and that the secondary processes having resonances that move to higher log ω with increasing temperature enhance the amplitude of the $Li^+$-hopping attempts where the resonances cross. The losses of the middle frequency are the largest. Since ionic hopping can be expected to give a larger loss than rotations of $(OLi)^-$ dipoles, we assign the loss at middle frequency to ionic transport and that at highest frequency to dipole rotations. The lowest frequency resonance that moves to higher frequencies with increasing temperature is associated with the glass surface.

In the Na-glass, the tan δ resonance at room temperature is broad below a glass transition temperature $T_g \approx 41°C$, but above $T_g$ the two resonances have a larger amplitude and can be distinguished; the maximum amplitude of the two resonances is in the interval between 61 °C and 129 °C. In this same temperature interval, the ionic conductivity, Fig. 6, is enhanced. Since the Arrhenius plots at $T < T_g$ and $T > 141$ °C connect with the same slope, we deduce that the enhancement of $\sigma_i$ varies as $(T - T_g)^{-1}$. The temperature interval of the enhancement of $\sigma_i$ is the same as the interval where the two tan δ frequencies have their closest approach and strongest enhancement of one another. At the lowest frequencies, the third resonance in the Na-glass tan δ spectrum appears to be associated with the glass surface as in the Li-glass. Here, also there is no evidence of a hydrogen bond resonance in samples reacted above 230 °C.

The self-charging process at open circuit of the symmetric Cu/Na-glass/Cu cell after a plating charge for 1 h, Fig. 8, reflects the fact that the metallic sodium plated on the anode current collector comes from the electrolyte; the cathode supplies electrons to the anode during charge, but it cannot supply $Na^+$ to the electrolyte. An electric double-layer capacitance (EDLC) is created at the cathode consisting of positive electron holes in the Cu conduction band and, in the electrolyte, a net negative charge resulting from the $Na^+$ depletion and any mobile anions. The cathode EDLC lowers the cathode Fermi energy, which makes it more difficult to plate sodium on the anode as the cathode EDLC increases with depletion of sodium from the electrolyte. During charge, the excess electron concentration in the anode may either react with

View Article Online
DOI: 10.1039/C5EE02924D



surface $Na^+$ ions from the electrolyte to plate sodium on the anode current collector or be trapped by surface $Na^+$ ions in an anode EDLC. Plating of sodium occurs on a Cu anode in the voltage range $2.4 \lesssim V \lesssim 3.0$ V, but formation of an anode EDLC appears to become competitive at voltages $V \gtrsim 3.4$ V, Fig. 7. Switching to open-circuit eliminates the applied voltage and traps excess electrons in the anode and an electron deficit in the cathode. The cell is no longer symmetric, and charge is transported inside the cell to equalize the electrochemical potentials of the two electrodes, thereby creating a cell self-charge to reach an equilibrium cell voltage. Electron transfer between the electrodes is blocked, but slower ionic motions are not blocked. The cathode EDLC suppresses $Na^+$ diffusion back to the cathode, but adjustment of the electrochemical potential can be made by transfer of $Na^+$ ions across the anode-electrolyte interface to plate sodium on the anode. This self-charge process has a built-in feedback since plating of sodium reduces the anode EDLC, which lowers the energy for the next surface-$Na^+$ to be plated. What is remarkable is that in the cell investigated, the rate of self-discharge is slowed in the interval $1.5 < V < 1.7$ V. The reproducibility of the change in rate of self-charge was not investigated. Instead, we investigated the process after a 15 h charge.

On increasing the charging time to over 15 h, a second Cu/Na-glass/Cu symmetric cell not only showed the voltage required for plating increases from 2.4 V to 3.0 V; but another process begins to compete above 3.0 V and may become dominant above 3.4 V. The thickness of the plated sodium layer after 8 h is calculated to be approximately 5 μm, which is similar to the rate of plating of other metals[4]. With our model for the self-charge process in Fig. 6, we argue that the observed plating current of +0.17 mA at a plating voltage of +2.4 V on switching to a discharge current of −0.10 mA reflects the role of the EDLC formed at charging voltages $V > 3.0$ V. Removal of electrons from the anode to the cathode by the discharge current lowers the cathode EDLC as well as the anode Fermi energy, but the self-charge process retains a positive cell voltage of 2.4 V because plating of surface $Na^+$ of the anode EDLC occurs as well as $Na^+$ diffusion back toward the cathode. The rate of Na plating at 2.4 V is slower than the rate of formation of the anode EDLC above 3.4 V, so the plating continues for 15 h after switching to a discharge current of −0.10 mA. A plating current of +0.17 mA is needed to give a +0.07 mA at the plating voltage 2.4 V after switching.

Fig. 10 shows the DC conductivity of a symmetric Li/Li-glass/Li cell during a 20 minute plating at 0.1 mA/cm$^2$ on one side before switching to plating in the opposite direction. The $\sigma_{DC}$

View Article Online
DOI: 10.1039/C5EE02924D



at 44 ºC is seen to improve over time; after 250 h, it is about 5 times smaller than the AC conductivity shown in Fig. 2. Since the AC conductivity measures the bulk $Li^+$ conductivity, it can be concluded from this experiment that the impedance to $Li^+$ transport across the Li-metal/Li-glass interface is acceptable and that the contact between the Li-glass electrolyte and plated metallic Li did not degrade with time. After 19 days of cycling, the cell broke down as a result of oxide formation on the Lithium interface with the current collector resulting from a poor glove box; there was no evidence of a problem resulting from formation of dendrites at the Li-glass/Li-metal interface.

## Conclusion

Precursors of the crystalline antiperovskites $A_3OCl$ phases with A = Li or Na can be rendered dry, glass/amorphous solid electrolytes by the addition of water up to its solvation limit with/without the addition of a small amount of $Ba(OH)_2$ or another oxide or hydroxide. The solvated water leaves the glass/amorphous solid product as gaseous HCl and the $(OH)^-$ as water above 230 ºC. Although the crystalline product from the antiperovskite precursors is $A_{3-x}H_xOCl$, there is no evidence of hydrogen bonding in the glass/amorphous products. The electron energy gap of the glass electrolyte is greater than 9 V; no XRD evidence for a disproportionation into $Li_2O$ and LiCl was found. Grinding the solid product under ethanol to obtain a paste for easy application to a large surface area avoids attack of the small-particle surfaces by the water of humid air. After incorporation of the glass-electrolyte slurry in a cell, the cell is sealed in Epoxy and the ethanol evaporates below 150°C through the wet Epoxy to allow the glass to reform as a continuous solid. Measurements of the $Li^+$ and $Na^+$ AC impedances of glass pellets have shown that both the Li-glass and the Na-glass have room-temperature conductivities comparable to those of the best liquid organic electrolytes. Chronopotentiometry measurements of the room-temperature DC $Li^+$ conductivity in a symmetric Li/Li-glass/Li cell, which includes transport across the Li-metal/Li-glass interface on cycling 20 min. each way, have shown that the impedance to $Li^+$ transfer across the Li-metal/Li-glass interface is acceptable with no degradation over 19 days of cycling at a rate of 0.1 mA $cm^{-2}$. The dielectric loss tangents show three resonances in their frequency spectra. The middle-frequency resonance is assumed to be the hopping attempt frequency of the diffusing alkali ion; it is enhanced in amplitude as the resonant frequency of another process crosses it. The anomalous charging behavior is accounted for by

View Article Online
DOI: 10.1039/C5EE02924D



formation of a cathode EDLC that forces an increase in the charging voltage of a Cu/Na-glass/Cu symmetric cell that is needed to maintain a fixed current; plating out of sodium at $2.4 \leq V \leq 3.0$ V changes to formation of an anode EDLC in the interval $3.0 < V < 3.4$ V. Above a glass-transition temperature $T_g = 41$ °C in the Na-glass, the $Na^+$ conductivity is enhanced where the resonant frequencies cross. In the Li-glass, the two high-frequency resonances overlap at room-temperature and no $T_g$ is observed above 28 °C in the AC conductivity. Constant-current charge voltages in symmetric Cu/Na-glass/Cu cells show plating of Na metal on a Cu current collector occurs at a voltage $V > 2.4$ V that increases with formation of an EDLC at the cathode until, above 3.4 V, formation of an EDLC at the anode competes with sodium plating to give a stronger increase in charging voltage with time. These features give rise to an anomalous self-charge on switching from a charging voltage to open-circuit and to a positive cell charging current with sodium plating on the anode in the presence of a −0.1 mA applied discharge current. Experiments with symmetric cells having alkali-metal electrodes demonstrate compatibility between the electrode and the electrolyte and a lowering with time of the impedance to alkali-metal transfer across the electrode/electrolyte interface.

**Acknowledgments**

We acknowledge support from the Robert A. Welch Foundation, Houston, Texas (grant No. F-1066) and the FCT - Portuguese project PTDC/CTM-ENE/2391/2014.

View Article Online
DOI: 10.1039/C5EE02924D



## References

1. P.B. Bruce, ed. Solid State Electrochemistry, Cambridge University Press 1995, Table 2.1, p. 24.

2. M.H. Braga, J.A. Ferreira, V. Stockhausen, J.E. Oliveira, A. El-Azab, *J. Mater. Chem. A.*, **2**, 5470 (2014).

3. H. Mehrer, ed. Diffusion in Solids Fundamentals, Methods, Materials, Diffusion-Controlled Processes, Springer Series in Solid-State Sciences, 1st edn, vol. 155, 2007.

4. M. Schlesinger, ed. Modern Electroplating, Wiley-Interscience publication, J. Wiley & Sons, Inc., 4th edn, 2000.